We conclude that differences in population variability were affected by the deterministic characteristics of the population dynamics as well as the stochastic factors (Fig. 3, C and D). These differences were in turn related to the position of the species along slow-fast continuum of life history variation (*3*, *5*, *6*) as expressed by r_1 (Fig. 3B). The relative contribution of the parameters describing the expected dynamics and stochastic factors to the population fluctuations is in solitary birds likely to be closely related to the type of demographic process, i.e., whether it is recruitment-driven or survival-restricted (Fig. 4). Fluctuations in the size of recruitment-driven populations are more strongly influenced by environmental stochasticity than survival-restricted populations. Consequently, reliable projections of avian populations will require precise estimates and modeling of stochastic as well as deterministic components of the dynamics. On the other hand, estimating the form of density dependence will be more important for predicting population fluctuations of long-lived species with high values of θ. Reliable estimates of the environmental stochasticity (*11*) as well as precise estimates of the carrying capacity (*21*) will require access to long-term time series with small sampling errors (*29*).

References and Notes

1. R. M. May, *Philos. Trans. R. Soc. London* **351**, 1951 (1999).
2. R. C. Lewontin, in *The Genetics of Colonizing Species*, H. G. Baker, G. L. Stebbins, Eds. (Academic Press, New York, 1965), pp. 77–91.
3. E. R. Pianka, *Am. Nat.* **104**, 592 (1970).
4. D. E. L. Promislow, P. H. Harvey, *J. Zool.* **220**, 417 (1990).
5. E. L. Charnov, *Life History Invariants* (Oxford Univ. Press, Oxford, 1993).
6. B.-E. Sæther, Ø. Bakke, *Ecology* **81**, 642 (2000).
7. T. R. E. Southwood, *J. Anim. Ecol.* **46**, 337 (1977).
8. C. W. Fowler, *Ecology* **62**, 602 (1981).
9. ———, *Evol. Ecol.* **2**, 197 (1988).
10. M. E. Gilpin, F. J. Ayala, *Proc. Natl. Acad. Sci. U.S.A.* **70**, 3590 (1973).
11. B.-E. Sæther *et al.*, *Am. Nat.* **151**, 441 (1998).
12. O. Diserud, S. Engen, *Am. Nat.* **155**, 497 (2000).
13. Supplementary material is available on *Science* Online at www.sciencemag.org/cgi/content/full/295/5562/2070/DC1.
14. We based our analyses on time series of populations of solitary bird species that have been censused for 15 or more years with no significant linear trend in population size with time and no population estimate of less than 10 pairs. To reduce the bias in the parameters because of large sampling errors in population estimates, we only included time series that were based on direct nest counts (e.g., hole nesters) or on the presence of a large number of color-ringed individuals. The population parameters were estimated by maximum likelihood methods. We modeled fluctuations in the size of the logarithm of the population fluctuations, $X = \ln N$, where N is the population size at time t. Let $\Delta X = \ln(N + \Delta N) - \ln(N)$ and σ_e^2 be the environmental stochasticity (*23*). We assume large enough population sizes to ignore any effects of demographic stochasticity. The distribution of ΔX, conditional on N, is assumed to be normal with mean $m(x) = r_m[1 - (N/K)^\theta]\Delta t$ and variance $\sigma_e^2\Delta t$. Here K is the carrying capacity, r_m is the mean specific growth rate, and θ describes the type of density regulation in the theta-logistic function (*10*) $m(x)$. The strength of the density regulation at K is then (*21*)

$$\gamma = r_m\theta = r_1\theta/(1 - K^{-\theta}),$$

where r_1 is the specific growth rate when $N = 1$. Thus, strong density regulation occurs at K when the population growth rate is high and/or for large values of θ. The parameters were estimated by maximum likelihood. The expected change in the logarithm of population size may be written as $E(\Delta X) = r_1\{1 - [(e^{X\theta} - 1)/(e^{\theta\ln(K)} - 1)]\} = \mu(X, K, \theta)$ for $\theta \neq 0$ and $E(\Delta X) = r_1[1 - (X/\ln K)]$ for $\theta = 0$ (*21*, *23*). The parameters are estimated by maximizing the likelihood function $L(K,\theta,\sigma_e^2) = \Pi^n f(X_{i+1}|X_i;K,\theta,\sigma_e^2)$, where $X_0 = K$, and $X_{i+1} = X_i + \Delta X_i$. The function $f(X_{i+1}|X_i; K, \theta, \sigma_e^2)$ is the normal distribution with mean $X_t + \mu(X_i, K, \theta)$ and variance σ_e^2. The uncertainty in the parameters was determined by simulating repeated data sets from the model, with the maximum likelihood estimates of the parameters, and then calculating bootstrap replicates from each simulation. Reliable estimates of r_1 are often difficult to obtain in stationary time series because the populations most of the time are found fluctuating around K (*24*). We therefore estimated this parameter by a standard Leslie matrix model (*6*) using available demographic information. We entered into the model maximum fecundity rate (number of offspring produced to independence per female) and the lowest age specific mortality rate recorded during the study period or in any age class. The estimates of r_1 obtained in this way were in nine bird species (*25*) closely correlated to bias-corrected values of r_1 obtained from time-series analyses (correlation coefficient = 0.73, $P < 0.05$, $n = 9$).
15. We assume that the parameters $(\theta, \ln \sigma_e^2)$ are binormally distributed among the species and that the estimates of these parameters are approximately binormally distributed for each species with parameters determined by the results of the parametric bootstrapping (*14*). Each pair of estimates $(\theta, \ln \sigma_e^2)$ will then have bivariate normal distributions. Estimates of the binormal variation among species are found by maximum likelihood.
16. C. W. Fowler, *Curr. Mammol.* **1**, 401 (1987).
17. T. Royama, *Analytical Population Dynamics* (Cambridge Univ. Press, Cambridge, 1992).
18. A problem in analyses of time series of population fluctuations is that the coefficient of variation increases with the census period (*26*, *27*) because of autocorrelations due to age structure effects, delayed density dependence, or autocorrelation in the environmental noise (*28*, *29*). However, from the diffusion approximation for the theta-logistic model, we can calculate the variance of the stationary distribution (*12*). If we assume the demographic variance σ_d^2 to be much less than the product of the carrying capacity K and environmental stochasticity σ_e^2, we can compute the variance of the stationary distribution of population sizes $\sigma_N^2 = K^2\Gamma[(\alpha + 2)/\theta]/[(\alpha + 1)/\theta]^{2/\theta}\Gamma(\alpha/\theta)$, where $\alpha = 2r_1/\sigma_e^2(1 - K^{-\theta}) - 1$, r_1 is the growth rate when $N = 1$, and Γ denotes the gamma function (*12*). Thus, σ_N^2 can be used to compare the variability in time series of different lengths. However, in the present data set, a close correlation was found between $\sigma_N 2$ and CV (correlation coefficient = 0.94, $P < 0.001$, $n = 13$).
19. I. Newton, *Population Limitation in Birds* (Academic Press, San Diego, 1998).
20. P. Arcese, J. N. M. Smith, W. M. Hochachka, C. M. Rogers, D. Ludwig, *Ecology* **73**, 805 (1992).
21. B.-E. Sæther, S. Engen, R. Lande, P. Arcese, J. N. M. Smith, *Proc. R. Soc. London Ser. B* **267**, 621 (2000).
22. R. Lande *et al.*, *Am. Nat.*, in press.
23. S. Engen, Ø. Bakke, A. Islam, *Biometrics* **54**, 840 (1998).
24. S. Aanes, S. Engen, B.-E. Sæther, T. Willebrand, V. Marcström, *Ecol. Appl.*, **12**, 281 (2002).
25. S. Engen, B.-E. Sæther unpublished data.
26. S. L. Pimm, *The Balance of Nature?* (Univ. of Chicago Press, Chicago, 1991).
27. A. Ariño, S. L. Pimm, *Evol. Ecol.* **9**, 429 (1995).
28. T. Coulson *et al.*, *Science* **292**, 1528 (2001).
29. O. N. Bjørnstad, B. T. Grenfell, *Science* **293**, 638 (2001).

30. We thank H. Weimerskirch and A. Dhondt for access to unpublished data and R. Lande and R. Aanes for critically reading a previous draft. Supported by the Research Council of Norway, the EU Commission (project METABIRD), and a grant from Programme International Cooperation Scientifique (CNRS) to B.-E.S.

7 December 2001; accepted 21 January 2002

The RAR1 Interactor SGT1, an Essential Component of *R* Gene–Triggered Disease Resistance

Cristina Azevedo,[1]* Ari Sadanandom,[1]* Katsumi Kitagawa,[2] Andreas Freialdenhoven,[3] Ken Shirasu,[1]† Paul Schulze-Lefert[1,3]

Plant disease resistance (*R*) genes trigger innate immune responses upon pathogen attack. RAR1 is an early convergence point in a signaling pathway engaged by multiple *R* genes. Here, we show that RAR1 interacts with plant orthologs of the yeast protein SGT1, an essential regulator in the cell cycle. Silencing the barley gene *Sgt1* reveals its role in *R* gene–triggered, *Rar1*-dependent disease resistance. SGT1 associates with SKP1 and CUL1, subunits of the SCF (Skp1-Cullin–F-box) ubiquitin ligase complex. Furthermore, the RAR1-SGT1 complex also interacts with two COP9 signalosome components. The interactions among RAR1, SGT1, SCF, and signalosome subunits indicate a link between disease resistance and ubiquitination.

Plant disease resistance (*R*) genes are key components in pathogen perception; *R* genes activate a battery of defense reactions, collectively called the hypersensitive response (HR) (*1*). A number of *R* genes from various plant species have been isolated and characterized in detail (*2*). Although different *R* genes confer resistance to a variety of pests, including bacteria, viruses, fungi, nematodes, and insects, many *R* gene products share common structural modules such as a nucleotide-binding site and a leucine-rich repeat domain. The structural sim-

ilarity among R proteins suggests the existence of common or related signal transduction mechanisms downstream of pathogen perception (*3*). Several genes required for *R* gene function have been identified, and some may represent such downstream signaling components. For example, *EDS1* encodes a lipase-like protein, and *NDR1* encodes a putative membrane-associated protein (*4*, *5*). However, the biochemical function(s) of these proteins remains to be elucidated.

Barley *Rar1* (*HvRar1*) was originally isolated as a gene required for resistance signaling triggered by multiple *R* genes, including *Mla6* and *Mla12*, which confer resistance to the pathogenic powdery mildew (*Blumeria graminis f. sp. hordei*) (*6*). *HvRar1* encodes a protein with two highly similar but distinct zinc-binding domains called CHORD-I and -II (cysteine- and histidine-rich domain). RAR1 homologs are present in plants, protozoa, metazoa, and fungi but are absent in yeast. The sequence and paired arrangement of CHORDs are highly conserved, a finding that suggests the preservation of a common biochemical function. Gene silencing of *Rar1* homologs in *Caenorhabditis elegans* perturbed specific developmental processes (*6*). In humans, a RAR1 homolog (melusin) was isolated as a muscle-specific protein that interacts in vitro with the cytoplasmic domain of integrin (*7*). This finding suggests that the conserved RAR1s are key components in diverse biological processes in eukaryotes.

To investigate the molecular function(s) of RAR1 in plants, we searched for interacting proteins by using a yeast two-hybrid screen in which *Arabidopsis* RAR1 (AtRAR1) served as bait (*8*). We identified two interacting proteins sharing extensive amino acid similarity to each other (87%) and to yeast SGT1 (48 and 50%, respectively), which we designated AtSGT1a and AtSGT1b (Fig. 1, A and C). HvRAR1 also interacts with both AtSGT1a and AtSGT1b, indicating that the SGT1-binding function of plant RAR1 proteins has been conserved in monocots and dicots. We also cloned an *Sgt1* homolog from barley (*HvSgt1*) by using reverse transcription–polymerase chain reaction (RT-PCR) with degenerate primers. Only a single sequence was identified; thus, barley probably contains only one copy of *Sgt1*. Both AtSGT1a and AtSGT1b are more similar to one another than to SGT1 proteins of monocots, suggesting that these two *Arabidopsis* homologs are the result of recent gene duplication. Alignments of amino acid sequences defined five domains in plant SGT1 proteins: a tetratricopeptide repeat domain (TPR) (*9*), two variable regions (VR1 and VR2), the CS motif (present in metazoan CHORD and SGT1 proteins), and the SGS motif (SGT1-specific motif) (Fig. 1B).

Deletion analysis in the yeast two-hybrid system revealed that the CS motif of AtSGT1a interacts with CHORD-II but not

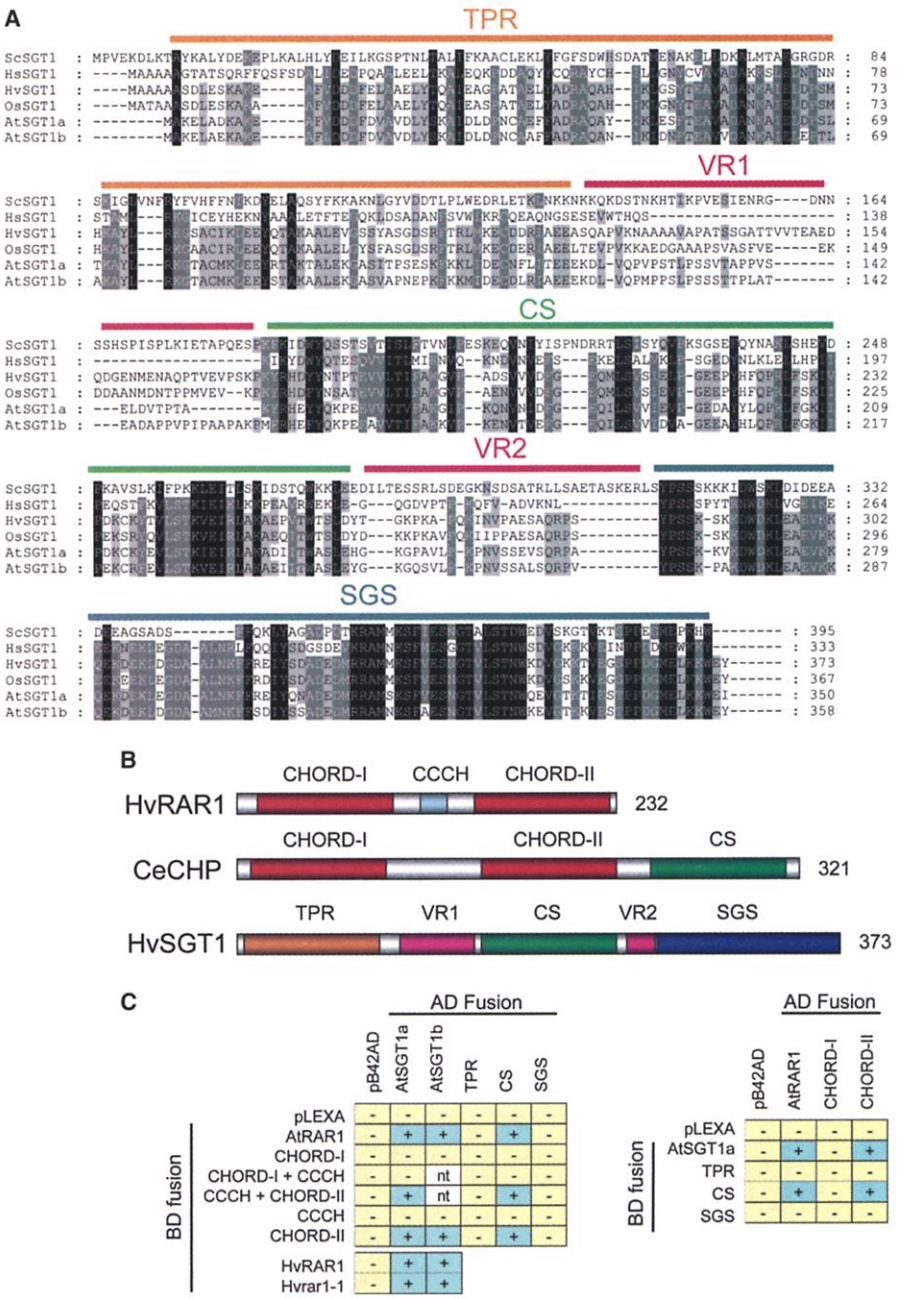

Fig. 1. The deduced SGT1 protein sequence and physical interaction between SGT1 and RAR1. (**A**) Sequence alignment of SGT1 proteins. Sc, *Saccharomyces cerevisiae*; Hs, human; Hv, barley; Os, rice; At, *Arabidopsis*. The black (100%), dark gray (80%), and light gray (60%) boxes represent levels of amino acid identity or similarity. GenBank accession numbers: HvSGT1, AF439974; AtSGT1a, AF439975; AtSGT1b, AF439976 (*22*). (**B**) Graphical representation of the structures of HvRAR1, CeCHP (Ce, *C. elegans*), and HvSGT1 domains. The numbers on the right indicate the number of amino acids per protein. (**C**) Yeast two-hybrid analysis of the interaction between SGT1 and RAR1. *HvRAR1*, *Hvrar1-1* (*6*), *AtRAR1*, *AtSGT1a*, *AtSGT1b*, and fragments of *AtRAR1* and *AtSGT1a* were amplified by PCR and cloned into the Eco RI and Xho I sites of the pLexA (binding domain fusion) or pB42AD (activator domain fusion) vectors, as indicated. Interactions were detected by induction (+) or no induction (–) of *lacZ* and *LEU2* reporter genes under the control of the *lexA* gene in yeast EGY48 cells; nt, not tested. TPR, tetratricopeptide repeat domain; VR1 and VR2, variable regions; SGS, SGT1-specific motif.

[1]The Sainsbury Laboratory, John Innes Centre, Colney Lane, Norwich NR4 7UH, UK. [2]Department of Molecular Pharmacology, St. Jude Children's Research Hospital, 332 North Lauderdale Street, Memphis, TN 38105-2794, USA. [3]Max-Planck-Institut für Züchtungsforschung, Abteilung Biochemie, Carl-von-Linne-Weg 10, D-50829 Köln, Germany.

*These authors contributed equally to this work.
†To whom correspondence should be addressed. E-mail: ken.shirasu@bbsrc.ac.uk

with CHORD-I or Cys-Cys-Cys-His (CCCH) of AtRAR1 (Fig. 1C). A single amino acid substitution in CHORD-I (*Hvrar1-1*) of HvRAR1 did not abolish interaction with AtSGT1, corroborating the finding that CHORD-II is sufficient for the RAR1-SGT1 complex formation (Fig. 1C). Thus, although the sequences of CHORD-I and CHORD-II are highly related, these domains may serve distinct roles. Interestingly, the CS motif of SGT1 proteins is also found at the COOH terminus of the metazoan RAR1 homolog, CHP (*6*) (Fig. 1B). Therefore, the RAR1-SGT1 interaction represents an example of the Rosetta Stone principle (*10*), whereby the presence of two domains in a single polypeptide in one species (in this case, CHORD-II and CS in metazoan CHP) indicates that the two domains interact with one another when they are present in separate proteins in another species. These results suggest that RAR1 and SGT1 participate in a related biochemical mechanism(s) in eukaryotic organisms that contain both genes.

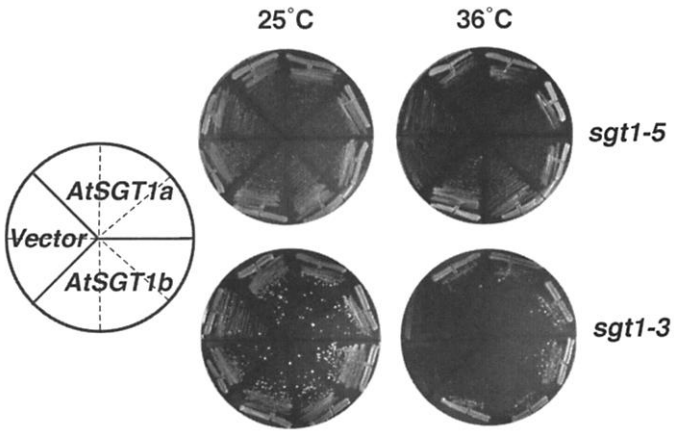

Fig. 2. *Arabidopsis SGT1a* and *SGT1b* complement the *sgt1* mutation in yeast. Yeast strains YKK57 (*sgt1-5*) and YKK65 (*sgt1-3*) were transformed with *AtSGT1a*, *AtSGT1b* (cloned into p426GAL), or vector p426GAL. The transformants were selected on Sc-Ura 2% glucose plates and spread on Sc-Ura 2% raffinose plates. The strains were spread on Sc-Ura 2% galactose plates and incubated for 4 days to test their ability to complement the temperature-sensitive *sgt1-5* and *sgt1-3* growth defects.

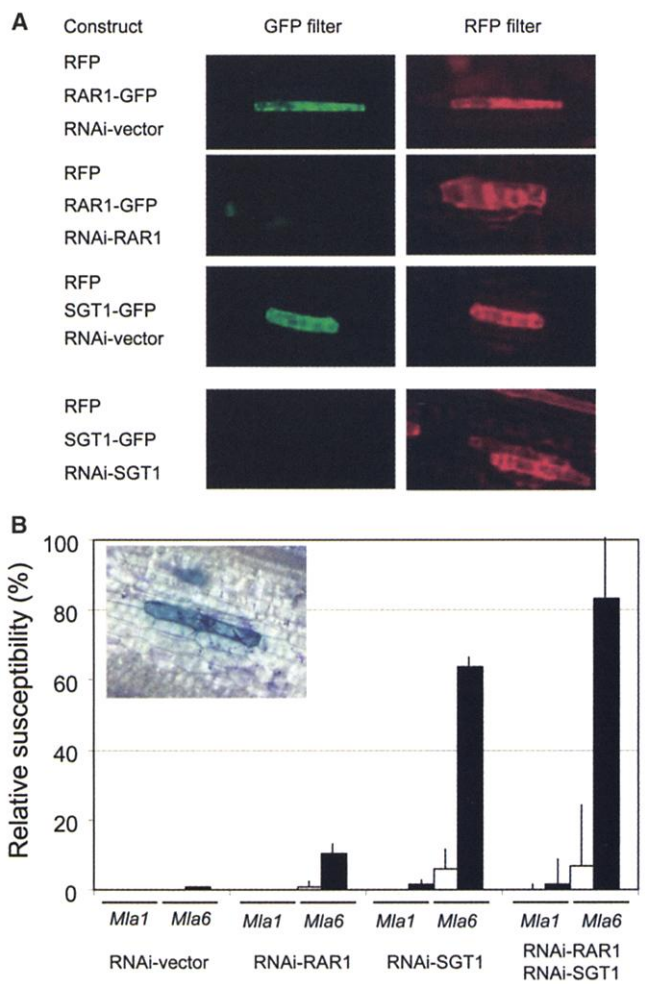

Fig. 3. *HvSgt1* is required for full resistance to powdery mildew triggered by *Mla6*. (**A**) dsRNAi was used to silence single-cell expression of *HvRar1* and *HvSgt1*. Detached barley leaves were bombarded with the constructs, as described (*23*). After 48 hours, transformed epidermal cells were identified using a microscope with the GFP or RFP filter. Magnification, ×300 (**B**) Effect of silencing of *HvRAR1* and *HvSGT1* on *Mla6*- and *Mla1*-resistance pathways in single cells. After particle-mediated delivery of corresponding dsRNAi constructs and the GUS marker plasmid, leaves were incubated at 20°C for either 48 hours (white bar) or 96 hours (black bar) before inoculation with powdery mildew spores. After 48 hours, samples were stained for GUS activity and fungal structures (with Coomassie blue). The fraction of susceptible GUS-positive cells in bombardments lacking a corresponding *R* gene construct but containing an empty dsRNAi vector was defined as 100% susceptibility (the control fraction). The relative susceptibility was then calculated as the fraction of susceptible GUS-positive cells bombarded with a test dsRNAi construct and an *R* gene, divided by the control fraction, ×100. (mean ± SD of three experiments). The inset (magnification, ×300) shows a typical susceptible leaf epidermal cell expressing GUS in which powdery mildew successfully formed an intracellular haustorium and initiated growth of aerial hyphae.

To determine whether HvSGT1 is essential in *R* gene–triggered disease resistance, we used a single-cell transient double-stranded RNA inhibition (dsRNAi) system for silencing the corresponding endogenous genes (*12*). In this assay, a DNA construct encoding an intron-spliced dsRNA is delivered via gold-coated particles into epidermal cells of barley leaves. A plasmid-expressing red fluorescent protein (RFP) was delivered with the test constructs to mark the transformed cells. To monitor the silencing efficiency, we cobombarded a third plasmid-expressing green fluorescent protein (GFP) fused to the COOH terminus of either HvRAR1 or HvSGT1. Forty-eight hours after delivery, the green fluorescence of cells expressing HvRAR1-GFP or HvSGT1-GFP was markedly reduced, whereas the levels of red fluorescence remained unchanged (Fig. 3A). This finding indicates that *HvSgt1* and *HvRar1* expression can be silenced in a sequence-dependent manner.

Next, we tested the effect of silencing *HvRar1* and *HvSgt1* in *Mla1*- and *Mla6*-specific disease resistance by inoculating bombarded leaves with spores of powdery mildew strains expressing the corresponding avirulence genes *AvrMla1* or *AvrMla6* (Fig. 3B). In these experiments, we used β-glucuronidase (GUS) as a marker for transformed cells. Silencing of *HvRar1* for 96 hours impaired the resistance triggered by *Mla6*, although only in 10% of the attacked epidermal cells, whereas *Mla1*-dependent resistance was not affected. This finding confirmed previous genetic and molecular analyses that indicated that *HvRar1* is required for *Mla6*-triggered

but not for *Mla1*-triggered resistance to powdery mildew (*13–15*). A reduction in *Mla6*-triggered resistance became apparent in *HvSgt1*-silenced cells 48 hours after bombardment and was more pronounced after 96 hours; at that time, about 63% of epidermal cells were rendered susceptible to attack by the A6 isolate containing *AvrMla6*. *Mla1*-triggered resistance in *HvSgt1*-silenced cells was largely unaffected (1.7%) even at 96 hours, indicating that *HvSgt1* is required for *Mla6*-specific but not for *Mla1*-specific resistance. When *HvRar1* and *HvSgt1* were cosilenced, *Mla6*-triggered resistance was highly disabled (83%). These results suggest cooperation between HvRAR1 and HvSGT1 in *Mla6*-triggered resistance. The minor, if any, contribution of HvRAR1 and HvSGT1 to *Mla1*-triggered resistance is surprising because MLA1 and MLA6 share 95% sequence identity (*14*, *15*). The minor contribution may indicate the existence of another signaling pathway for MLA1. Alternatively, a signal emitted from MLA1 may be stronger than the signal emitted from MLA6, and it may require only residual amounts of HvRAR1 and HvSGT1 to transmit signals to downstream components.

To examine whether HvSGT1 and HvRAR1 also interact in planta, we used antibodies to HvRAR1 and HvSGT1 for coimmunoprecipitation experiments with leaf extracts of barley plants grown in the absence of pathogens. Anti-HvRAR1 immune complexes from wild-type plants contained HvSGT1, which was not detected in *rar1-2* plants (Fig. 4). In a reciprocal experiment, HvRAR1 was detected in HvSGT1 complexes; this finding confirms that in the absence of pathogens in planta, HvRAR1 associates with HvSGT1.

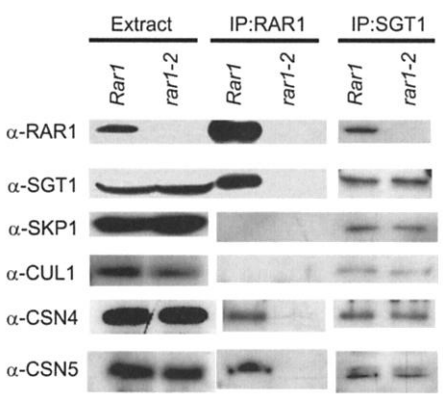

Fig. 4. HvSGT1 interacts with HvRAR1, SCF, and COP9 siganalosome subunits in vivo. Extracts from wild-type *Rar1* or mutant *rar1-2* barley plants were immunoprecipitated with antibodies to RAR1 or SGT1. Samples of eluted fractions (40 μl) were analyzed by immunoblotting with antibodies to RAR1, SGT1, SKP1 (*24*), CUL1 (*25*), CSN4, and CSN5 (Affiniti, Exeter, UK).

In yeast, SGT1 associates with the kinetochore complex and the SCF-type (Skp1-cullin–F-box) E3 ubiquitin ligase by interacting with SKP1 (*11*). Immunoblotting analysis confirmed that HvSGT1 complexes contained SKP1 homolog(s) (Fig. 4). CUL1 homolog(s), another subunit of the SCF ubiquitin ligase, was also detected in the HvSGT1 immunoprecipitates. Interestingly, the association between HvSGT1 and these subunits also occurs in *rar1-2* mutant plants. Because neither SKP1 nor CUL1 homolog(s) was detected in the HvRAR1 immunoprecipitates, at least two distinct HvSGT1 complexes may exist, one containing the subunits of the SCF ubiquitin ligase and the other containing HvRAR1.

Recently, the COP9 signalosome was shown to directly interact with SCF E3 ubiquitin ligases (*16*, *17*). This finding prompted us to investigate the possible interaction between the HvRAR1-HvSGT1 complex and COP9 subunits CSN4 and CSN5. Analyzing HvRAR1 and HvSGT1 immunoprecipitates with antibodies to CSN4 and CSN5 revealed the presence of barley CSN4 (HvCSN4) and CSN5 (HvCSN5) in the HvRAR1-HvSGT1 complex from wild-type *Rar1* plants (Fig. 4). HvCSN4 and HvCSN5 were also detected in HvSGT1 immunoprecipitates from *rar1*-2 mutant plants; this result indicates that HvSGT1 associates with HvCSN4 and HvCSN5 independently of HvRAR1.

By its interaction with SCF complexes, the yeast protein SGT1 exerts its essential activity in the degrading of SIC1 (a Clb5/cdc28 kinase inhibitor) and CLN1 (a G_1 cyclin) (*11*). Recent studies have also shown that mouse SGT1 is associated with the SCF^{Skp2} complex (*16*). Thus, one possible role of plant SGT1 could be to target resistance-regulating proteins for degradation by the 26*S* proteasome via specific SCF complexes. In this scenario, the target proteins would be negative regulators of disease resistance.

SCF E3 ubiquitin ligases can modify protein activity. For example, monoubiquitination regulates membrane transport, subcellular localization, transcription, and protein kinase activity (*18*). Thus, the SGT1 complex may participate in modification of protein activity or may have a dual role for activation and degradation of the target via ubiquitination. Such a dual role of ubiquitination has been reported in the regulation of transcriptional activation (*19*). In this context, the *R* gene product itself could be a target of the SGT1 complex for activation and degradation. Indeed, the R protein RPM1 rapidly degrades during the resistance response (*20*). This may lead to receptor desensitization that could restrict the HR to a small number of host cells at sites of attempted pathogen invasion.

What is the role of the RAR1-SGT1 interaction in disease resistance? Because yeast does not contain RAR1 homologs, RAR1 itself cannot be required for SCF E3 ligase function, per se. The presence of HvCSN4 and HvCSN5 in the HvRAR1-HvSGT1 complex suggests a link to the COP9 signalosome, which is closely related to the lid complex of the 26*S* proteasome (*21*). RAR1 could connect, via SGT1, the COP9 signalosome to SCF E3 ubiquitin ligases to promote ubiquitination of still unknown target(s) in *R* gene–mediated signal transduction. Future systematic single-cell silencing experiments of SCF and COP9 signalosome components in combination with protein interaction studies should provide more detailed insights into the role of these complexes in *R* gene–specified disease resistance.

References and Notes

1. B. Baker, P. Zambryski, B. Staskawicz, S. P. Dinesh-Kumar, *Science* **276**, 726 (1997).
2. J. L. Dangl, J. D. G. Jones, *Nature* **411**, 826 (2001).
3. K. Shirasu, P. Schulze-Lefert, *Plant Mol. Biol.* **44**, 371 (2000).
4. K. S. Century *et al.*, *Science* **278**, 1963 (1997).
5. A. Falk *et al.*, *Proc. Natl. Acad. Sci. U.S.A.* **96**, 3292 (1999).
6. K. Shirasu *et al.*, *Cell* **99**, 355 (1999).
7. M. Brancaccio *et al.*, *J. Biol. Chem.* **274**, 29282 (1999).
8. Supplemental material is available on *Science* Online at www.sciencemag.org/cgi/content/full/1067554/DC1.
9. G. L. Blatch, M. Lassle, *Bioessays* **21**, 932 (1999).
10. E. M. Marcotte, M. Pellegrini, M. J. Thompson, T. O. Yeates, D. Eisenberg, *Nature* **402**, 83 (1999).
11. K. Kitagawa, D. Skowyra, S. J. Elledge, J. W. Harper, P. Hieter, *Mol. Cell* **4**, 21 (1999).
12. P. Schweizer, J. Pokorny, P. Schulze-Lefert, R. Dudler, *Plant J.* **24**, 895 (2000).
13. J. H. Jörgensen, *Genome* **39**, 492 (1996).
14. D. Halterman, F. Zhou, F. Wei, R. P. Wise, P. Schulze-Lefert, *Plant J.* **25**, 335 (2001).
15. F. Zhou *et al.*, *Plant Cell* **13**, 337 (2001).
16. S. Lyapina *et al.*, *Science* **292**, 1382 (2001).
17. C. Schwechheimer *et al.*, *Science* **292**, 1379 (2001).
18. C. M. Pickart, *Mol. Cell* **8**, 499 (2001).
19. S. E. Salghetti, A. A. Caudy, J. G. Chenoweth, W. P. Tansey, *Science* **293**, 1651 (2001).
20. D. C. Boyes, J. Nam, J. L. Dangl, *Proc. Natl. Acad. Sci. U.S.A.* **95**, 15849 (1998).
21. C. Schwechheimer, X. W. Deng, *Trends Cell Biol.* **11**, 420 (2001).
22. Single-letter abbreviations for the amino acid residues are as follows: A, Ala; C, Cys; D, Asp; E, Glu; F, Phe; G, Gly; H, His; I, Ile; K, Lys; L, Leu; M, Met; N, Asn; P, Pro; Q, Gln; R, Arg; S, Ser; T, Thr; V, Val; W, Trp; and Y, Tyr.
23. K. Shirasu, K. Nielsen, P. Piffanelli, R. Oliver, P. Schulze-Lefert, *Plant J.* **17**, 293 (1999).
24. A. Ferrando, R. Farras, J. Jasik, J. Schell, C. Koncz, *Plant J.* **22**, 553 (2000).
25. J. C. del Pozo, M. Estelle, *Proc. Natl. Acad. Sci. U.S.A.* **96**, 15342 (1999).

26. We thank M. Estelle for providing the CUL1 antibody, C. Koncz for the SKP1 antibody, C. Casais for technical support, R. Wise for *Mla6* genomic sequence, and L. Jones and N. Collins for critical reading of the manuscript. Supported by grants from the Gatsby Charitable Organization (K.S. and P.S.L.) and the UK Biotechnology and Biological Sciences Research Council (P.S.L.) and a Ph.D. fellowship from Fundação para a Ciência e a Tecnologia (C.A.).

30 October 2001; accepted 15 January 2002
Published online 14 February 2002;
10.1126/science.1067554
Include this information when citing this paper.